Two-dimensional semiconductor $HfSe_2$ and $MoSe_2/HfSe_2$ van der Waals heterostructures by molecular beam epitaxy

Cite as: Appl. Phys. Lett. **106**, 143105 (2015); https://doi.org/10.1063/1.4917422
Submitted: 04 February 2015 • Accepted: 01 April 2015 • Published Online: 08 April 2015

K. E. Aretouli, P. Tsipas, D. Tsoutsou, et al.

Two-dimensional semiconductor $HfSe_2$ and $MoSe_2/HfSe_2$ van der Waals heterostructures by molecular beam epitaxy

K. E. Aretouli, P. Tsipas, D. Tsoutsou, J. Marquez-Velasco, E. Xenogiannopoulou, S. A. Giamini, E. Vassalou, N. Kelaidis, and A. Dimoulas[a)]
Institute of Nanoscience and Nanotechnology, National Center for Scientific Research "Demokritos," 15310, Aghia Paraskevi, Athens, Greece

(Received 4 February 2015; accepted 1 April 2015; published online 8 April 2015)

Using molecular beam epitaxy, atomically thin 2D semiconductor $HfSe_2$ and $MoSe_2/HfSe_2$ van der Waals heterostructures are grown on AlN(0001)/Si(111) substrates. Details of the electronic band structure of $HfSe_2$ are imaged by *in-situ* angle resolved photoelectron spectroscopy indicating a high quality epitaxial layer. High-resolution surface tunneling microscopy supported by first principles calculations provides evidence of an ordered Se adlayer, which may be responsible for a reduction of the measured workfunction of $HfSe_2$ compared to theoretical predictions. The latter reduction minimizes the workfunction difference between the $HfSe_2$ and $MoSe_2$ layers resulting in a small valence band offset of only 0.13 eV at the $MoSe_2/HfSe_2$ heterointerface and a weak type II band alignment. © *2015 AIP Publishing LLC*. [http://dx.doi.org/10.1063/1.4917422]

The advent of stable 2D atomically thin transition metal dichalcogenide semiconductors offers exciting possibilities for nanoelectronic device scaling and extends our options to a number of low power versatile applications.[1] Up to now, the group VIB metal dichalcogenide ($(Mo,W)X_2$) atomically thin semiconductors with a *2H* crystal structure have been studied extensively and their great potential to impact nanoelectronics has been demonstrated on the basis of field effect transistors (FETs) and generic integrated circuits.[2,3] However, the rather low carrier mobilities (as compared to conventional semiconductors Si and Ge) and the difficulties to grow uniform large area films inhibit their use in several applications. Other 2D semiconductors[4] as, for example, group IVB metal dichalcogenides ($(Zr,Hf)X_2$)[5] with a *1T* crystal structure and potentially better properties need to be investigated. $HfSe_2$, in particular, is predicted[6–8] to be an indirect gap semiconductor with a measured bulk value of $Eg \sim 1.1$ eV, similar to Si,[9,10] and a remarkably high phonon-limited mobility of $\sim 3500\ cm^2/V{\cdot}s$ at room temperature.[11]

The existence of a large number of 2D materials with similar crystal structure but with diverse electronic band structure properties including energy gap, electron affinities, workfunction (WF), etc., allows for the formation of high quality van der Waals heteroepitaxial materials combinations with abrupt interfaces and a variety of band alignments offering flexibility for the design of (opto)electronic devices. A particularly interesting type II band alignment has been predicted to occur[6] in group IVB/VIB metal dichalcogenide heterostructures (e.g., $MoSe_2/HfSe_2$), allowing for the realization of 2D vertical staggered or broken gap tunnel FETs (TFETs).[12] However, experimental band alignments may deviate from theoretical values due to possible surface induced modification of workfunctions and charge transfer effects at the interface. In recent work on $HfSe_2$ films grown on HOPG and MoS_2 by molecular beam epitaxy (MBE),[13] the measured workfunction of $HfSe_2$[13] is substantially smaller than the theoretically reported value[6] implying that deviations from the predicted band alignments with group VIB materials[6] are to be expected too. This calls for a deeper investigation of epitaxial $HfSe_2$ films and their heterostructures with other 2D dichalcogenides with the aim to examine the band alignment configuration and the potential impact on nanoelectronic applications.

In the present work, we report on MBE-grown $HfSe_2$ and $MoSe_2/HfSe_2$ heterostructures. The growth is performed on wide-gap-AlN(0001)/Si(111) technologically important substrates. We focus on issues related to the van der Waals epitaxial growth employing structural and physical characterization as well as first principles calculations. We emphasize on valence band imaging in *k*-space and band alignment determination which is correlated with possible surface modifications due to Se adatoms.

The optimum temperature for the growth of $HfSe_2$ films on top of the AlN/Si(111) substrates was investigated in the 225 °C–690 °C range. The surface ordering and crystalline quality of the substrate and the epilayers are controlled *in-situ* by RHEED (Fig. 1). An optimum two-step growth is employed for $HfSe_2$[14] resulting in excellent crystallinity along with a flat surface from 1 up to 6 ML $HfSe_2$ epilayers, as evidenced by the distinct elongated streaks (Figs. 1(b) and 1(c)).

A different set of $MoSe_2/HfSe_2$ heterostructure samples is produced where a $HfSe_2$ is first grown at the optimum conditions described above, followed by $MoSe_2$ deposition at the optimum conditions described elsewhere.[14,15] It should be noted here that reversing the order of the epitaxy such that the $MoSe_2$ is grown first on AlN followed by $HfSe_2$ overgrowth is also an option. However, emphasis is given on the direct order ($MoSe_2/HfSe_2$/AlN) because $MoSe_2$ is much more stable in air against oxidation[15] compared to $HfSe_2$[13] and essentially serves as a protective cap during processing of the bilayer for device fabrication.

Despite the large lattice mismatch between the different epitaxial layers and the substrate, all RHEED streaks are

a)Author to whom correspondence should be addressed. Electronic mail: a.dimoulas@inn.demokritos.gr

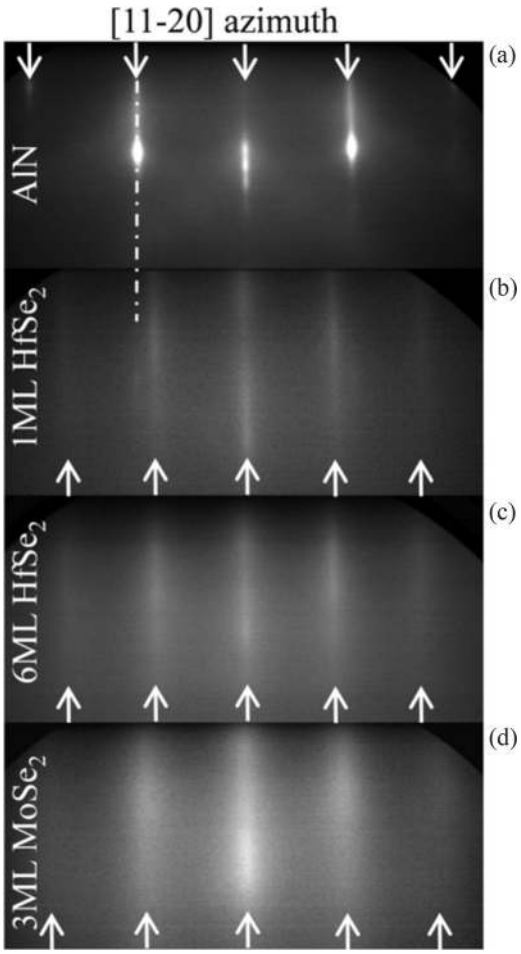

FIG. 1. RHEED pattern along [11–20] azimuth of (a) 200 nm metal organic chemical vapor deposition (MOCVD) AlN(0001)/Si(111), (b) 1 ML $HfSe_2$/AlN/Si(111), (c) 6 ML $HfSe_2$/AlN/Si(111), and (d) 3 ML $MoSe_2$ on $HfSe_2$.

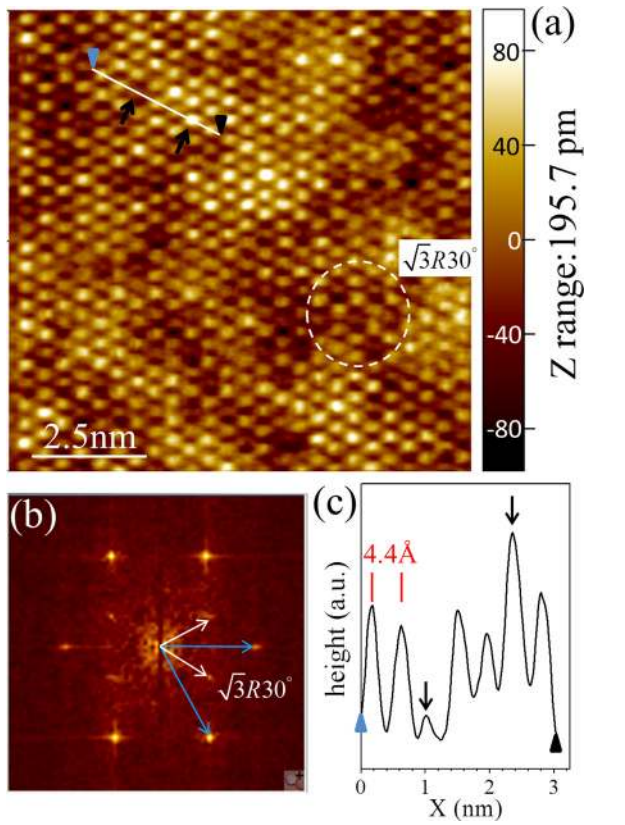

FIG. 2. (a) Room temperature high resolution UHV-STM image of 1 ML $HfSe_2$ on AlN(0001)(10 nm × 10 nm, $U_{bias} = 0.5$ V, I = 0.5 nA). (b) The corresponding FFT pattern revealing two groups of spots with hexagonal symmetry. Blue arrows indicate a periodicity of 4.4 Å, while the white arrows indicate a $\sqrt{3} \times \sqrt{3}R30^\circ$ periodicity with respect to the other, which corresponds to the superstructure marked by dashed circle in (a). (c) Profile along the line in image (a) marking the positions where surface (ad)atoms are either missing or exceeding from the surface.

azimuthially aligned (Fig. 1), suggesting that the epilayers are epitaxially grown such that $[11–20]_{MoSe_2}//[11–20]_{HfSe_2}//[11–20]_{AlN}$ in the plane. Since no additional streaks are observed, it can be inferred that there are no rotated 30° or 90° domains, indicating that the epilayers are highly oriented single crystals. Comparing the distance between the streaks of the $MoSe_2$ and $HfSe_2$ epilayers with the ones of the AlN substrate, the lattice constant of the $MoSe_2$ and $HfSe_2$ hexagonal lattices is estimated to be ∼3.26 Å and ∼3.78 Å, very close to reported bulk values,[6,7,16] indicating the absence of strain as would be expected in van der Waals heteroepitaxy[17,18] of these materials.

The surface of thin (1 ML) $HfSe_2$ films on AlN is investigated *in-situ* by room temperature UHV-STM. A high resolution image along with the diffractogram (Fourier pattern) and a line scan are given in Fig. 2. A surface hexagonal lattice is evident with a lattice constant $\alpha_s = 4.4$ Å which is higher than the lattice constant $\alpha_{(HfSe_2)} = 3.79$ Å of $HfSe_2$. This leads to the assumption that an ordered hexagonal adlayer with larger lattice constant partially covers the $HfSe_2$ surface, affecting also electron diffraction (see slightly blur RHEED pattern in Fig. 1). In addition, a faint $\sqrt{3} \times \sqrt{3}R30^\circ$ structure appears in the Fourier pattern (Fig. 2(b)). It is anticipated that unstable adatoms separated by a distance of $\sqrt{3}a_s$ are either located at a higher point from the surface or completely missing, revealing $HfSe_2$ atoms underneath as can be seen also in the line scan of Fig. 2(c). This creates the $\sqrt{3} \times \sqrt{3}R30^\circ$ pattern in the real image as seen in Fig. 2(a) (dashed circle). In a larger scale, the missing adatoms at $\sqrt{3}a_s$ positions produce a darker contrast in about 50% of the scanned area. The rest 50% with brighter contrast can be interpreted as fully formed adlayer with hexagonal lattice. A profound candidate for the adlayer is selenium condensed on the surface during cooling down; the assumption of Se adlayer is supported by Density Functional Theory (DFT) calculations.[14] Energy minimization using Perdew-Burke-Ernzerhof (PBE) potentials with van der Waals corrections indicates that the most stable position of the Se adatom is on top of Hf, while the second best position is on top of a Se atom of the $HfSe_2$ surface. A Se adatom initially placed on top of Se in the bottom layer of $HfSe_2$ is not stable reverting, after relaxation, to a position on top of a surface Se. Adsorption of two Se adatoms is energetically favored with binding energy of −2.17 eV per Se adatom yielding a stable configuration as shown in Fig. 3, in line with the observed hexagonal arrangement in STM real image (Fig. 2(a)). The empty center of the dashed hexagon in Fig. 3 reflects the unstable location of Se adatoms on top of a Se at the bottom of $HfSe_2$ and can be correlated with the missing (or higher-lying) Se adatoms inferred from STM (Figs. 2(a) and 2(c)).

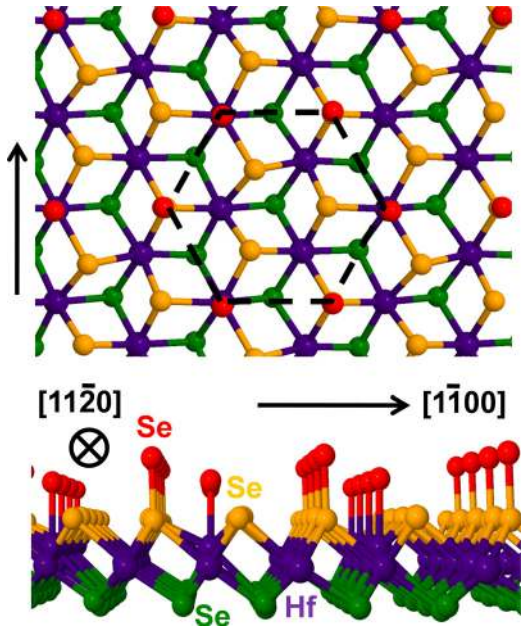

FIG. 3. Top and side view of the Se adlayer structure on $HfSe_2$ as produced by first principles (DFT) calculations. The dashed line marks the hexagonal arrangement of Se adatoms separated between each other by a distance of 4.4 Å on average.

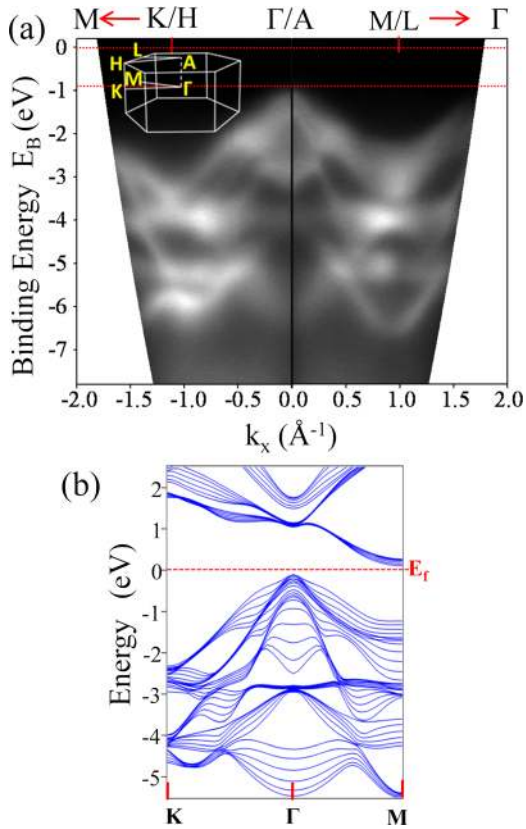

FIG. 4. (a) ARPES valence band imaging using He I excitation of 21.22 eV along the high symmetry directions K/H-Γ/A-M/L of the Brillouin zone for a 6 ML $HfSe_2$/AlN sample. (b) DFT band structure calculations of 6 ML $HfSe_2$ free-standing slab with spin orbit coupling.

The excess surface-adsorbed Se bonded to Hf (Fig. 3) is compatible with the slight over stoichiometry (Se/Hf ratio around 2.1/1 on average) estimated from our *in-situ* XPS measurements.[14] Nevertheless, Se-Se bonds could not be resolved from the Se 3d core level because we are at the limits of our energy resolution of our XPS system.

The $HfSe_2$ electronic valence band structure for a 6 ML film is imaged along high symmetry crystallographic directions of the Brillouin zone (BZ) using *in-situ* angle resolved photoelectron spectroscopy (ARPES) (Fig. 4(a)). Using PBE potentials with van der Waals corrections, where the spin-orbit interaction is taken into account, first principles calculations for 6 ML $HfSe_2$ slab are performed and the results are shown in Fig. 4(b). The agreement between theory and experiment for the valence band dispersions is remarkably good, showing that the valence band maximum (VBM) is located at the center of the Brillouin zone (Γ point). Theory predicts (Fig. 4(b)) that the conduction band minimum (CBM) is located at the edge of the BZ (M point) yielding an indirect gap semiconductor with $E_g = 0.2$ eV. Deviations from previous published works are attributed to the different parameters of calculations [e.g., inclusion of spin orbit coupling (SOC) and layer thickness].[6,19] Assuming that E_F is located at zero binding energy in Fig. 4(a), as it is usually the case, the experimental energy gap is estimated to be larger than 0.9 eV which is in line with the measured $E_g \sim 1.1$ eV in bulk[9] and epitaxial[13] $HfSe_2$ films. Similar valence band structure is imaged for the 1 ML $HfSe_2$/AlN, whereas in the case of capped $HfSe_2$ with $MoSe_2$, the $HfSe_2$ layer cannot be resolved as ARPES is an extremely surface sensitive method especially when performed with 21.22 eV excitation energy, as in our case. The well-defined dispersion curves along the crystallographic directions shown in Fig. 4(a) support the conclusions drawn on the basis of RHEED data that the film is well oriented in plane with no rotational domains which, if existed, could produce a mixed, ill-defined image in Fig. 4(a).

Following the growth of 6 ML of $HfSe_2$ on AlN, additional $MoSe_2$ layers are grown sequentially so as to obtain material with thicknesses of 1, 2, 3, 4, and 8 ML of $MoSe_2$. Analysis of Mo 3*d* and Se 3*d* XPS peaks[14] indicates stoichiometric $MoSe_2$ films at any thickness. Once each thickness target is reached, growth is interrupted to measure low energy electron cut-off, valence band maxima, and core levels by UPS and XPS. Representative spectra near the cut-off regions are given in Fig. 5(a) for two thick $HfSe_2$ and $MoSe_2$ layers. For $HfSe_2$, both techniques yield the same value of WF ~ 5.5 eV. In the case of $MoSe_2$, UPS and XPS yield slightly different values of 5.1 and 5.2 eV, respectively. The difference of 0.1 eV in workfunction values is attributed to experimental error. The measured values for $HfSe_2$ are notably lower compared to our theoretical estimates of 5.9 eV (Fig. 5(b)) for bare $HfSe_2$ and the previously reported theoretical value of 5.94 eV.[6] They also deviate substantially from the experimental value of 4.4 eV reported in Ref. 13. Note, however, that our experimental WF = 5.5 eV agrees well with the theoretical value of 5.59 eV (Fig. 5(b)) for the $HfSe_2$/Se adlayer system, indicating that Se adsorption on $HfSe_2$ surface inferred from Figs. 2 and 3 may be an explanation for the lower experimental WFs observed. The measured $MoSe_2$ WF of 5.1–5.2 eV agrees reasonably well with our calculated value of 5.44 eV;[14] however, it deviates substantially from the theoretical value of 4.57 eV reported

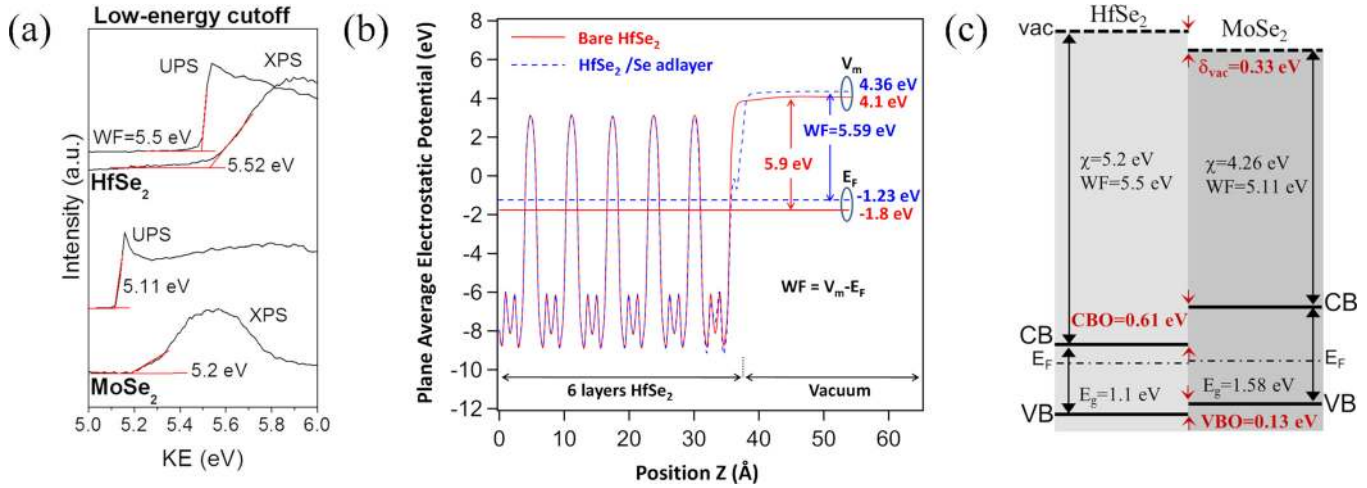

FIG. 5. (a) Low energy cut off for the thick $HfSe_2$ and $MoSe_2$ samples, as determined from both XPS and UPS measurements, (b) plane averaged electrostatic potential V as a function of the distance Z in the direction of growth, calculated by DFT. The work function is calculated as $WF = V_m - E_F$, where V_m is the maximum potential in vacuum, (c) schematic of the $MoSe_2/HfSe_2$ band offsets. χ denotes the electron affinity. E_g is the energy gap, while CBO and VBO denote the conduction and valence band offsets, respectively.

earlier. [6] Discrepancies between different theoretical results may be partly due to the different thicknesses assumed.

The energy separations[14] between the core levels and the VBM are used to calculate the valence band offset (VBO) and the band alignments (Fig. 5(c)) employing Kraut's method[20] and experimental literature values for the energy gaps.[9,13] The energy position of the Fermi level is compatible with the measured VBM and workfunction values of the two materials and they are compatible with electron affinity rule except from a vacuum level mismatch $\delta_{vac} = 0.33$ eV which may be partly due to the experimental uncertainties in measuring the $MoSe_2$ WF and the energy position of E_F. The band alignment results between $HfSe_2$ and $MoSe_2$ in Fig. 5(c) indicate a small VBO of only 0.13 eV and a weak type II band alignment. These results differ from the theoretical ones[6] which predict a type III heterojunction such that the VBM of $MoSe_2$ is at the same level or even higher than the CBM of $HfSe_2$. The main reason for the deviation between the present experimental results and predictions is that the experimental WF difference and hence the electron affinity difference of the two materials are much less than theoretical estimates. Although a type III heterojunction for broken gap TFETs is not confirmed, a type II band alignment at the interface, similar to the one observed in the WSe_2/MoS_2 system,[21] is possible, implying that atomically thin p-n heterojunctions[22] can be realized for staggered gap TFETs and for several applications in (opto)electronics.

In summary, $HfSe_2$ and $MoSe_2/HfSe_2$ van der Waals heterostructures are grown epitaxially on AlN(0001)/Si(111) by MBE with very high quality as evidenced from RHEED and ARPES imaging of the electronic band structure. By sampling the surface with UHV-STM, evidence is obtained of an ordered Se adlayer in hexagonal formation at least in parts of the surface, supported by first principles calculations. This adlayer could explain the UPS measured values of the $HfSe_2$ workfunction, which were found to be lower than the theoretically predicted ones. The band alignments at the $MoSe_2/HfSe_2$ heterointerface do not confirm a type III band alignment previously predicted by theory but they do show the tendency to form a weak type II interface in a p-n heterojunction configuration with prospective applications in (opto) electronics.

This work was financially supported from ERC Advanced Grant No. SMARTGATE-291260 and the Greek Program of EXCELLENCE (ARISTEIA)-TOP ELECTRONICS-745. The authors thank IMEC, Belgium, for providing the AlN/Si substrates.

[1]Q. H. Wang, K. Kalantar-Zadeh, A. Kis, J. N. Coleman, and M. S. Strano, Nat. Nanotechnol. **7**, 699 (2012).
[2]B. Radisavljevic, M. B. Whitwick, and A. Kis, ACS Nano **5**, 9934 (2011).
[3]H. Wang, L. Yu, Y. H. Lee, Y. Shi, A. Hsu, M. L. Chin, L. J. Li, M. Dubey, J. Kong, and T. Palacios, Nano Lett. **12**, 4674 (2012).
[4]A. K. Geim and I. V. Grigorieva, Nature **499**, 419 (2013).
[5]M. Chhowalla, H. S. Shin, G. Eda, L.-J. Li, K. P. Loh, and H. Zhang, Nat. Chem. **5**, 263 (2013).
[6]C. Gong, H. Zhang, W. Wang, L. Colombo, R. M. Wallace, and K. Cho, Appl. Phys. Lett. **103**, 053513 (2013).
[7]A. H. Reshak and S. Auluck, Physica B **363**, 25 (2005).
[8]H. Jiang, J. Chem. Phys. **134**, 204705 (2011).
[9]C. Gaiser, T. Zandt, A. Krapf, R. Serverin, C. Janowitz, and R. Manzke, Phys. Rev. B **69**, 075205 (2004).
[10]A. Aruchamy, *Photoelectrochemisty and Photovoltaics of Layered Semiconductors* (Kluwer Academic Publisher, 1992), p. 322.
[11]W. Zhang, Z. Huang, W. Zhang, and Y. Li, Nano Res. **7**, 1731 (2014).
[12]M. Li, D. Esseni, G. Snider, D. Jena, and H. G. Xing, J. Appl. Phys. **115**, 074508 (2014).
[13]R. Yue, A. T. Barton, H. Zhu, A. Azcatl, L. F. Pena, J. Wang, X. Peng, N. Lu, L. Cheng, R. Addou, S. McDonnell, L. Colombo, J. W. P. Hsu, J. Kim, M. J. Kim, R. M. Wallace, and C. L. Hinkle, ACS Nano **9**, 474 (2015).
[14]See supplementary material at http://dx.doi.org/10.1063/1.4917422 for details on the growth and on the DFT calculations, XPS of $HfSe_2$ and MoSe2, and XPS to calculate band offsets by Kraut's method.
[15]E. Xenogiannopoulou, P. Tsipas, K. E. Aretouli, D. Tsoutsou, S. A. Giamini, C. Bazioti, G. P. Dimitrakopulos, Ph. Komninou, S. Brems, C. Huyghebaert, I. P. Radu, and A. Dimoulas, "High quality large area $MoSe_2$ and $MoSe_2/Bi_2Se_3$heterostructures on AlN(0001)/Si(111) substrates by molecular beam epitaxy," Nanoscale (published online).
[16]R. Coehoorn, C. Haas, J. Dijkstra, C. J. F. Flipse, R. A. de Groot, and A. Wold, Phys. Rev. B **35**, 6195 (1987).
[17]F. S. Ohuchi, B. A. Parkinson, K. Ueno, and A. Koma, J. Appl. Phys. **68**, 2168 (1990).

[18]B. A. Parkinson, F. S. Ohuchi, K. Ueno, and A. Koma, Appl. Phys. Lett. **58**, 472 (1991).
[19]S. Lebegue, T. Bjorkman, M. Klintenberg, R. M. Nieminen, and O. Eriksson, Phys. Rev. X **3**, 031002 (2013).
[20]E. Kraut, R. Grant, J. Waldrop, and S. Kowalczyk, Phys. Rev. Lett. **44**, 1620 (1980).
[21]M.-H. Chiu, C. Zhang, H. W. Shiu, C. Chuu, C.-H. Chen, C.-Y. S. Chang, C. Chen, M. Chou, C. Shih, and L. Li, "Determination of band alignment in transition metal dichalcogenides heterojunctions," e-print arXiv:1406.5137.
[22]C.-H. Lee, G.-H. Lee, A. M. van der Zante, W. Chen, Y. Li, M. Han, X. Cui, G. Arefe, C. Nuckolls, T. F. Heinz, J. Cao, J. Hone, and P. Kim, Nat. Nanotechnol. **9**, 676 (2014).